J. Am. Soc. Mass Spectrom. (2014) 25:1332–1345
DOI: 10.1007/s13361-014-0885-0

RESEARCH ARTICLE

Electrospray Ionization Mechanisms for Large Polyethylene Glycol Chains Studied Through Tandem Ion Mobility Spectrometry

Carlos Larriba,[1,2,3] Juan Fernandez de la Mora,[1] David E. Clemmer[2]

[1]Mechanical Engineering Department, Yale University, New Haven, CT 06520, USA
[2]Department of Chemistry, Indiana University, Bloomington, IN 55455, USA
[3]SEADM, Parque Tecnológico de Boecillo, 47151 Boecillo, Valladolid, Spain

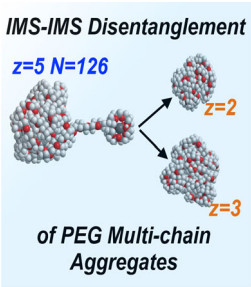

Abstract. Ion mobility mass spectrometry (IMS-MS) is used to investigate the abundance pattern, $n_z(m)$ of Poly-(ethyleneglycol) (PEG) electrosprayed from water/methanol as a function of mass and charge state. We examine $n_z(m)$ patterns from a diversity of solution cations, primarily dimethylammonium and triethylammonium. The ability of PEG chains to initially attach to various cations in the spraying chamber, and to retain them (or not) on entering the MS, provide valuable clues on the ionization mechanism. *Single chains* form in highly charged and extended shapes in most buffers. But the high initial charge they hold under atmospheric pressure is lost on transit to the vacuum system for large cations. In contrast, *aggregates of two or more chains* carry in all buffers at most the Rayleigh charge of a water drop of the same volume. This shows either that they form via Dole's charge residue mechanism, or that highly charged and extended aggregates are ripped apart by Coulombic repulsion. IMS-IMS experiments in He confirm these findings, and provide new mechanistic insights on the stability of aggregates. When collisionally activated, initially globular dimers are stable. However, slightly nonglobular dimers projecting out a linear appendix are segregated into two monomeric chains. The breakup of a charged dimer is therefore a multi-step process, similar to the Fenn-Consta polymer extrusion mechanism. The highest activation barrier is associated to the first step, where a short chain segment carrying a single charge escapes (ion-evaporates) from a charged drop, leading then to gradual field extrusion of the whole chain out of the drop.

Key words: Mass spectrometry, Ion mobility, PEG, Polyethyleneglycol, Poly(ethyleneglycol), Poly ethylene-glycol, Electrospray, Ionization, Polymer, Charge residue, Ion evaporation, Extrusion, Ethylammonium, Dimethylammonium, Dimers, Chains, Beads on a string, Dole's, Drift tube, DMA, IMS-IMS, Tandem IMS, Charge reducing buffer

Received: 7 December 2013/Revised: 2 March 2014/Accepted: 3 March 2014/Published online: 13 June 2014

Introduction

The mechanism of electrospray ionization (ESI) of long polymer chains differs considerably from that of either (i) large globular proteins or (ii) small ions, and is, as a result, not as well understood. This theoretical dearth, combined with the wide distribution of masses m and charge states z typical of electrosprayed polymers, has made the practical mass spectrometric (MS) analysis of polymers by ESI-MS far less successful than that of most other analytes. Early electrohydrodynamic ionization EHDI studies based on electrospraying glycerol solutions in vacuum had shown the presence of relatively small multiply charged polyethylene glycol (PEG) ions [1]. In view of the lack of drop evaporation in vacuo, it was that these small PEG ions were released by ion evaporation [2] directly from the liquid drop into the vacuum. Fenn and colleagues [3] later exploited a variety of atmospheric pressure electrospray ionization observations in support of the notion that PEG ions of arbitrarily large molecular weight may be produced by a peculiar multi-step mechanism where a short chain segment bearing one cation first jumps from the drop into the gas (ion-evaporation), and

Electronic supplementary material The online version of this article (doi:10.1007/s13361-014-0885-0) contains supplementary material, which is available to authorized users.

Correspondence to: Carlos Larriba; *e-mail:* clarriba@umn.edu

then pulls out the whole chain. Additional evidence in favor of the ion evaporation mechanism has been given by the groups of Consta and Konermann, first via numerical simulations [4–6], and more recently through a model quantifying the process of gradual PEG extrusion from the drop following the initial evaporation of an individual ion tied to the chain [7]. We shall for brevity refer to this model as the *Fenn-Consta* or the *extrusion* model, for which there is so far little experimental evidence. In the present study we continue a long tradition of making inferences on ionization mechanisms based on the measured distribution of ion abundance $n_z(m)$ as a function of charge state z and mass m (e.g., see Hogan et al. [8]). The complex two-dimensional (z,m) dependence is resolved here by combined use of ion mobility spectrometry and mass spectrometry (IMS-MS). The circumstance that one of the two IMS instruments used operates at atmospheric pressure also permits distinguishing between the original charge state z of an ion as electrosprayed, and its final value z' after one or several charge stripping events z→z' take place at the vacuum interface of the mass spectrometer. We use Collision Induced Dissociation to study the ionization of single PEG chains, as well as the stability of globular and nonglobular agglomerates of several chains (dimers, trimers, …), produced from concentrated solutions. To further study the possible ionization mechanisms, we vary the cation attaching to the chain among the following: H^+, NH_4^+, dimethylammonium$^+$ ($Met_2NH_2^+$), triethylammonium (Et_3NH^+), diethylammonium ($Et_2NH_2^+$), tripropylammonium ($Prop_3NH^+$), and tetrabutylammonium (But_4N^+). We will show that the drastically different mass spectra obtained from different buffers is largely due to loss of charge at the MS interface, rather than to differences in the ionization mechanism. Studying ionization mechanisms through MS alone is therefore risky. Irrespective of the buffer used, single chains seem to be produced predominantly as the highly stretched high-z ions observed in most previous studies, although the charge and structure configuration actually detected in the MS is often quite different due to the aforementioned charge loss within the MS. In contrast, PEG ions containing two or more chains seem to originate as partially folded or globular entities and are most likely charged residues apparently produced by Dole's mechanism [9], occupying charge states below the Rayleigh charge [10] of a water drop of the same volume [11]. The lack of highly stretched aggregates will be interpreted as supporting the *extrusion* mechanism. The sharp contrast between the stabilities of globular and non-globular dimers will be used to confirm further that drawing a polymer ion from either a solvent drop or a polymer melt is a multi-step process akin to the Fenn-Consta mechanism [3–6], with the highest activation energy being associated to the initial step of ejecting a short singly-charged polymer segment.

Experimental

Two experimental systems were used, both with their own advantages. The first system consists of an atmospheric pressure interfaced mobility spectrometer known as a differential mobility analyzer (DMA; SEADM model P4, resolution ~50–60) coupled to a quadrupole-TOF mass spectrometer (MDS SCIEX model QStarXL, *m/z* up to 40 kDa) [8,12].

The second system consists of a low pressure 3-m long He drift region with IMS-IMS-IMS capabilities in series with a time of flight (TOF) mass spectrometer. Both systems have been previously described and only a brief explanation will be given. A sketch of both systems is also provided in Figure S1 in the Supplementary Information.

Differential Mobility Analyzer

The DMA is a narrow band filter that transmits to the MS ions of a single mobility. Mobility classification is achieved by fixing the voltage difference between the two parallel plates of the DMA, and passing a gas (dry air) between the plates (downward in the figure). This disperses spatially into a fan the ions entering through the first slit, such that only those within a narrow mobility range pass through the second slit and are driven by the sample flow into the inlet orifice of the mass spectrometer. A mass spectrum is acquired at each mobility, while scanning over the mobility (by varying the voltage) results in a set of mass spectra, which are stored as a single DMA-MS file. The total duration of a full 2D scan varies between 5 and 60 min and can take up to several thousand different mass spectra. Unless otherwise indicated, zero declustering voltage (voltage difference between the inlet orifice and the skimmer) is used in order to minimize charge loss of the polymer ions at the MS interface. Data were processed with the help of SCIEX's Analyst QS program complemented with SEADM's two-dimensional graphical software plotting the detected ion signal (*intensity* from here on) versus *m/z* and V_{DMA} (or inverse mobility, see below) as a contour plot (see e.g., Figure 1). The color scale assigned to the ion intensity variable is logarithmic, which permits distinguishing signals over three orders of magnitude smaller than the maximum.

The voltage difference V_{DMA} across the two plates of the DMA is inversely proportional to ion mobility Z,

$$Z = k/V_{DMA} \tag{1}$$

through a proportionality constant k that depends on the flow rate of gas, and which we determine by calibration with the tetraheptyl-ammonioum cation dimer (Z_s=0.984 cm^2/Vs at room temperature [13]). The calibration voltages in the four most characteristic spectra shown were: 2394 V for PEG 11 K seeded with ammonium acetate (NH_4Ac), 1588 V and 1810 V for PEG 6 K and PEG 11 K seeded with dimethylammonium formate (Met_2NH_2F), and 1620 V for PEG 6 K seeded with triethylammonium formate (Eth_3NHF).

IMS-IMS-IMS Drift Tube (DT-MS)

In the case of a drift tube cell, a sample of ions is pulsed into a drift region at specified intervals. A homogeneous electric

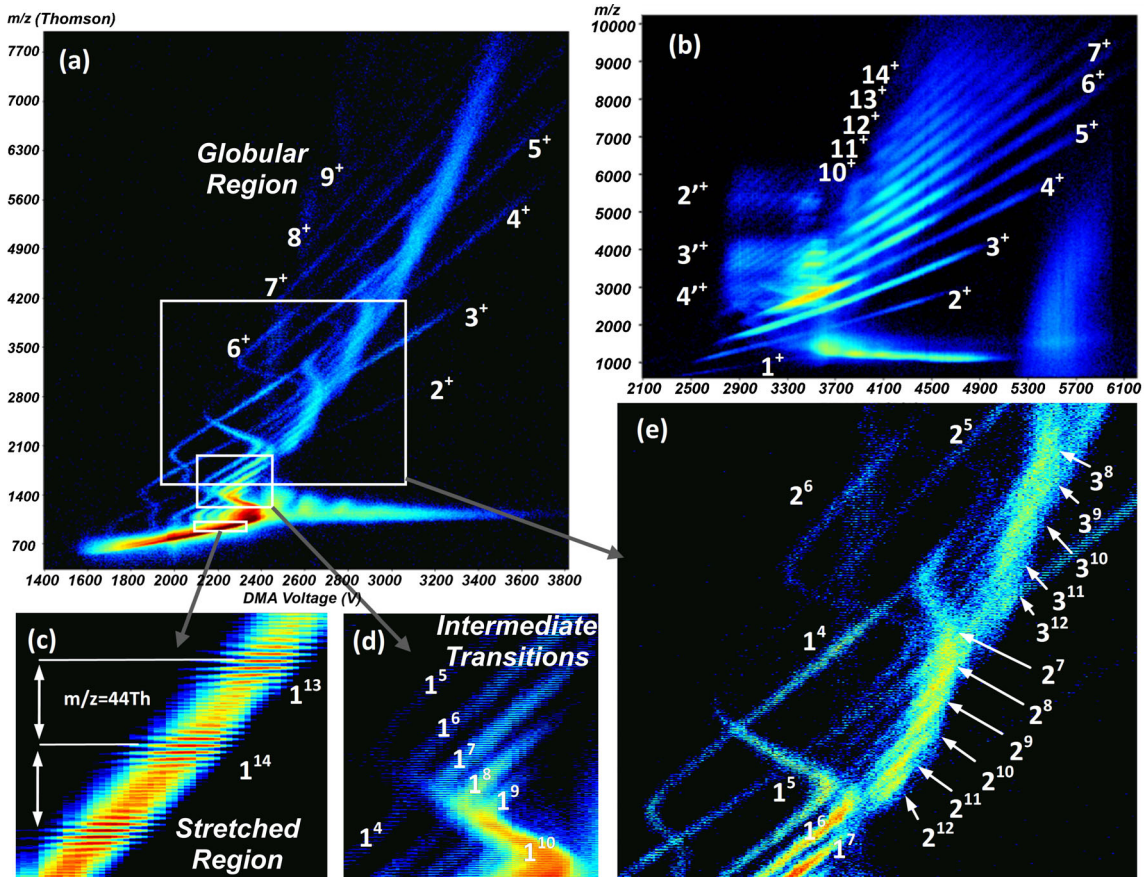

Figure 1. DMA-MS spectra for PEG 11 k electrosprayed from a 10 mM buffer of Met_2NH_2F **(a)**, or Eth_3NHF **(b). (c)**–**(e)** Zoom of selected regions in **(a)**. The notation x^z indicates the level of aggregation (x-mer) and the charge state z

field carries the ions through the length of the drift region and mobility-differentiated ions are separated through their interaction with the neutral gas. The total drift time can thus be measured for each particular ion and the electrical mobility calculated in inverse proportion to the drift time t_D [14–16]:

$$Z = k'/t_D, \tag{2}$$

where in this case k′ stands for the ratio between distance of travel and electric field. A 3-m drift tube can reach resolutions in excess of 100.

Multiple ion funnels, gates, and ion activating regions separating drift tube regions allow for tandem (or triple) IMS to be used [15,16]. Mobility ions separated in a previous drift region can be singled out and collision-dissociated before being transmitted to a second drift region for further study of the mobility of the fragments similarly to the way tandem MS works, albeit in this case the separation is done through collision cross section divided by charge (Ω/z) rather than mass over charge (m/z). Each drift region is labeled as D1, D2, or D3 in the Supplementary Figure S1b and separated by a funnel (labeled F), which helps concentrate the diffusion-broadened beam, and by an ion activation region (labeled IA) and a pulsing gate.

Finally, the drift tube is coupled to a TOF where the m/z of the analytes is obtained. A 2D contour plot very similar to that of the DMA-MS experimental apparatus can be procured by dividing the drift time window into bins of a specified width and acquiring different m/z data for every bin. For every pulse of ions burst into the drift region, a new contour plot is conformed and added to previous ones. Several thousand pulses are needed to obtain reasonable signals. Scan times vary in this case from 1 to 60 min, where each initial pulse takes approximately 30–80 ms.

Since the electric field can vary slightly from one acquisition to another, it is preferable to use a calibrant to obtain k′. The calibrant used for these sets of experiments is the most abundant doubly charged bradykinin ion, with a drift time of 21.1 ms and a CCS of 246A^2 [17].

Analytes

Charged ions were produced from a solution of 50/50 water-methanol with the addition of 10–30 mM of several buffer salts, including protons H^+ (from acetic acid), NH_4^+(from its acetate), $Met_2NH_2^+$, Met_3NH^+, $Eth_2NH_2^+$, Eth_3NH^+, and $Prop_3NH^+$ (from the five corresponding formates), and tetrabutylammonium But_4N^+ (from the But_4NCl). All salts are meant to increase the conductivity of the sample,

whereas the use of different salts aims at controlling the level of charging of the ions. Several PEG samples were used with average molecular weights, M_w, of 6, 6.6, 11, and 20 kDa. PEG 6 kDa was from Fluka (Saint Louis, MO, US) (used only in IMS-IMS). PEG 6.6 kDa was from Stepan (Northfield, IL, US) (used in DMA-MS). PEG 20 kDa was from Fluka and PEG 11 kDa (labeled 14 kDa) from Sigma Aldrich (Saint Louis, MO, US). Concentrations of PEG varied from 10 to 200 μM. Ammonium acetate (NH_4Ac) was from Sigma Aldrich.

In the case of the DMA, samples were introduced into a 1.5 mL polypropylene vial, which was pressurized to push the solution through a Polymicro silica capillary (i.d.: 41 μm o.d.: 360 μm) to a tapered tip of approximately 80 μm o.d. The capillary needle was placed a few hundred μm from the DMA inlet slit and centered in order to achieve maximum sensitivity. A small counterflow (~0.1–0.2 lpm) of dry air was passed from the DMA inlet slit into the ES chamber, which increased evaporation of the solvent and limited the introduction of uncharged or low mobility particles into the analysis region.

In the case of the drift tube, a pulled capillary tip and a syringe pump were used with a flow rate of approximately 10 μL/h. The capillary was placed several millimeters away from an inlet orifice 2 mm in diameter. A metal capillary tube of 30 cm was placed downstream of the orifice and connected the high pressure orifice with a low pressure region. The first funnel F1 separates this low pressure region from the drift tube, which is filled with He and kept at ~3 Torr.

A floating EMCO (Sutter Creek, CA, US) (DMA) or BERTAN (SPELLMAN HIGH VOLTAGE, Hauppauge, NY, US) (drift tube) HV power supply is used to bring the electrosprayed solution to a high voltage with respect to the front plate. This voltage difference forms a Taylor cone anchored at the tapered capillary tip. The electrospray is easily stabilized at a current of a few hundred nA. The stability of the electrospray is crucial in the case of the DMA as the ions are drawn directly inside the separation region but it is not as critical in the case of the drift tube as a funnel and a gate accumulate ions before pulsing them.

Results

Figure 1 shows two DMA-MS spectra of PEG 11 kDa (Figure 1a–b) as well as various insets (Figure 1c–e). We first focus on the upper left section (a), obtained from a 10 mM buffer of $Met_2NH_2^+$. The 2D spectrum is representative of the behavior of PEG ions from solutions containing small cations that bind strongly to the chain. A larger more detailed version of this and several other plots are provided in the Supplementary Information (Figure S2). The main features of these 2D spectra have been previously discussed in detail [18], and will be only briefly summarized. The many individual ion peaks present in DMA-MS spectra are naturally organized in colored features that visually appear as continuous because of the relatively small spacing between adjacent mass peaks ($\Delta m/z$ = 44 Da/z). Each of these features will be referred to as a *band*, and corresponds to a fixed charge state z and a discretely varying mass. The region colored in red and yellow labeled Stretched Region on the lower left side of (a) [see detail in (c)] is not a single band, being rather formed by a multitude of bands coalescing almost into each other. This region contains most of the ion signal, and corresponds to highly stretched ions [18–21]. Their mobility Z is approximately proportional to z and inversely proportional to the chain length (mass), whereby mobility ($Z \sim m/z$) and m/z separation are accordingly strongly correlated, and the ion signal collapses approximately into one rather than two dimensions. Towards the center and right end of (a) we see well-defined blue bands with positive slopes, labeled z^+ with their corresponding charge state. As long as these various bands remain approximately straight with positive slopes, they are associated to globular ions [18,19,22]. For each z, there is a minimum m/z below which the band undergoes a sharp bend [see (e) for details on some bends], corresponding to the first of a series of shape transitions, where the globular form ceases to be stable (labeled as intermediate transitions in the figure). The complex series of such transitions arising in each band is reasonably well understood [18], corresponding to diverse families of shapes defined through the competition of Coulombic repulsion between excess charges and cohesive attraction via Van Der Waals forces. The structure formed is always composed of a globule containing z-y elementary charges and a linear appendix (or two) containing the remaining y charges. At constant z, reducing the chain length (proportional to m) increases y up to $y = z$ (beads on a string or fully stretched configuration), whereas increasing chain length decreases y, leading eventually to a fully globular ion ($y = 0$) [23]. We observe no visible structural difference of the ions when using different concentrations of the solvents but we make no assumption on the critical stability and maximum charge of the ions for solvents other than 50/50 water/methanol. For a more comprehensive study on charge-induced stabilities for different solvents, we refer the reader to [24].

Even more informative than the DMA-MS spectrum with $Met_2NH_2^+$ is its comparison with the corresponding spectra in the Eth_3NH^+ buffer, shown in Figure 1b for PEG 11 k, and in Figure 2a for PEG 6.6 kDa. Comparatively low PEG charge states z achieved with triethylamine or other amine vapors added in the gas phase have been previously reported [24,25]. We also observe a greatly increased signal of low charge state ions, evident through the abundance of signal in the globular region, with no obvious signs of the many kinks or the fully stretched region that were so prominent with $Met_2NH_2^+$. However, what in the pure mass spectrum of Huang et al. [25] (similar to the MS projected on the left of Figure 2) appears as a simple low-z charging pattern is in reality considerably more complex, involving stretched configurations and charge states as high as those in $Met_2NH_2^+$. The first symptom for this more complex picture can be seen in the many secondary bands above and to the

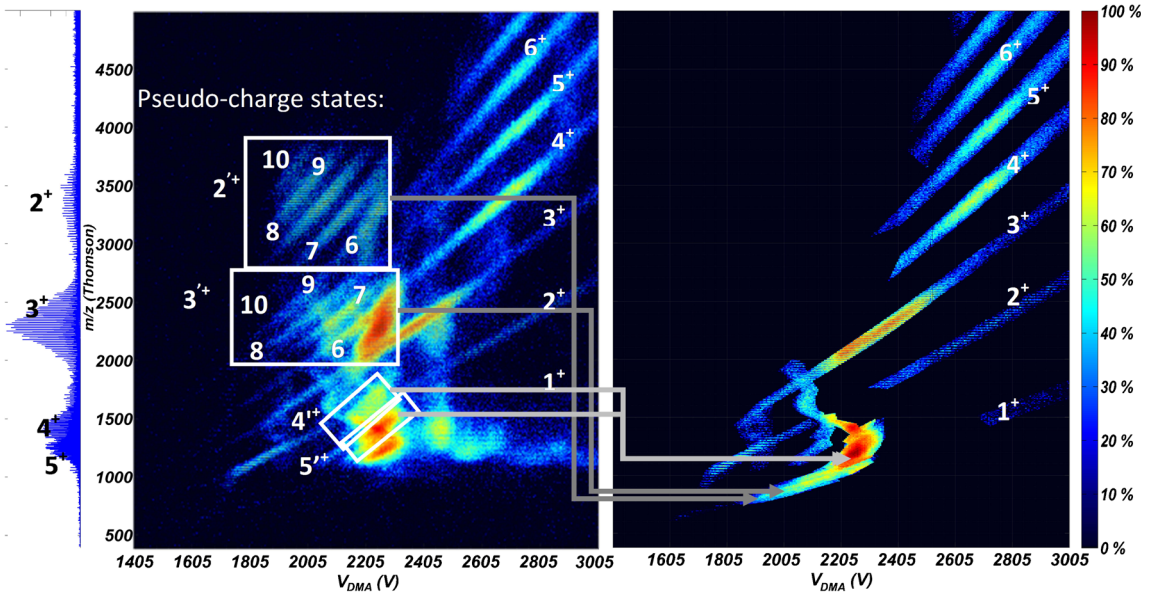

Figure 2. Detail of the DMA-MS spectrum for PEG 6.6 k in a Eth_3NH^+ buffer, similar to the low *m/z* high mobility region of Figure 1b. The spectrum on the left is uncorrected for numerous $z \rightarrow z'$ charge loss transitions taking place on the vacuum interface of the MS, resulting in different charge states in the DMA (z) and the MS (z′). The figure in the right corrects for these transitions by transforming the measured *m/z′* variable of unstable product ions into the original *m/z* value of corresponding parent ions, therefore showing ion abundances as produced by the electrospray process. The full contour plot is shown in an inset on the right figure

left of the bands for globular ions, labeled $2'^+$, $3'^+$, and $4'^+$ in Figure 1b. These bands do not appear in Figure 1a for $Met_2NH_2^+$and deserve some attention. We shall refer to them as "spurious" or "unnatural" because the mass *m* and corresponding low *z* values observed in the MS are utterly incompatible with the corresponding high mobilities measured in the DMA for any of the known structures of PEG. The spuriousness of some peaks is also clear from the fact that they appear for some buffers and not for others (i.e., no spurious peaks are evident in the data for $Met_2NH_2^+$ shown in Figure 1a or in Figure S2 of the Supplementary Information), and that the positions of the mass peaks associated to a given DMA voltage depend on the setting of the declustering voltage at the MS inlet. Peaks originating at a given ion mobility in the DMA and ending at an unnatural *m/z* in the MS have been observed numerous times in DMA-MS studies, and result in most cases from loss of charge at the entry of the MS. We therefore interpret these spurious ions as attributable to charge stripping from an original charge state *z* in the DMA to a lower charge state *z′* at the point where *m/z′* is measured in the MS. Conversely, we shall refer to the position of a peak in a DMA-MS spectrum as "original" when the ion has not undergone any stripping process between the DMA and the MS measurement.

A picture very similar to that of Figure 1b is seen in magnified form in Figure 2a for PEG 6.6 k. Here, a dominant (yellow-reddish) feature in the spectrum is centered at 2200*m/z*, in the globular region of the $z = 3^+$ band, corresponding to the nominal average molecular weight of the polymer sample (~6600 Da). However, "spurious" bands are also prominent in this figure, and can be accounted for as due to charge loss events $z \rightarrow z\text{-}1$ taking place multiple times as the ions are activated on entering the vacuum interface of the MS. The IMS and MS measurements therefore correspond to different ions, which as a result occupy "unnatural" positions in the DMA-MS spectrum. Significantly, these "spurious" ions do not appear in the drift tube-MS (DT-MS) because the pressure differential region primarily responsible for charge stripping is located right before the IMS region, and the apparatus remains blind to such processes (as will be shown in the sections below).

We now proceed to determine the original charge state of the unstable ions of Figures 1b and 2, in order to reconstruct the IMS-MS spectrum they would have formed had they been stable. The most notorious "spurious" ions in Figure 2a have been enclosed in boxes. The total signal from these boxes corresponds to most of the signal that appears in the MS spectrum (to the left of Figure 2a). Let us refer to the charge state determined in the MS for product ions of the transition $z \rightarrow z'$ as the pseudo-charge state *z′*, and reserve the term charge state *z* for the original ion charge in the DMA. The top left box corresponds (based on the *m/z* spacing of 22 Thomsons between subsequent ions) to pseudo-charge state $z' = 2$, and is accordingly labeled $2'^+$ in the figure. The multitude of bands present inside this first box suggest that each band corresponds to a different original charge state *z*. Their high mobility also indicates that the corresponding

parent ions most likely originate in the highly stretched region previously discussed in Figure 1a for $Met_2NH_2^+$, in which the *z*-bands are almost coincident for all charge states. Accordingly, to a first approximation, the many precursor ions transforming (at given mobility) into the many product ion bands with $z' = 2$ have approximately the same original *m/z*. Now, because the original *m/z* is approximately fixed, and

$$\frac{m}{z} = \frac{m}{z'}\frac{z'}{z}, \tag{2}$$

the *m/z′* values observed in this series are approximately related to each other through multiplication by rational numbers z/z′. The corresponding integer numbers *z* can hence be determined without ambiguity. In this case, with $z' = 2$, they happen to be z=7, 8, 9, 10, as labeled in Figure 2(a). The correctness of the inferred *z* values may be verified many times over by using different *m/z′* sequences obtained at different voltages. This procedure then gives the original *z*, whereby each mass peak in the box can be relocated at its original *m/z*, as done in the reconstructed IMS-MS spectrum in Figure 2b. The reconstruction routine brings all the bands almost on top of each other (and by chance also on top of charge state 1) as shown in Figure 2b. The magnitude of the loss of charge is striking, some product ions holding only 20% of their original charge (going originally from z = 10 to $z' = 2$). Pseudo-charge state $z' = 3$ falls on the same region, and can be treated analogously. A similar inversion can be implemented for the higher pseudo-charge states $z' = 4$–5, providing an assignment of the original *z* and *m* for each product ion identified. Pseudo-charge states 4 and 5 fall instead at the beginning of the folding transitions shown in Figure 2d [18]. $z' = 6$ is not varied since it falls directly on $z = 6$. The same reconstruction can be applied to PEG 11 kDa in Figure 1b (not shown).

Figure 3 quantifies the ion abundance, $n_z(m)$, previously displayed visually in the color scale of Figure 2b (PEG 6.6 k with Eth_3NH^+ buffer). See the Supplementary Information for a more detailed plot of the raw data (FigureS3). In particular, Figure 3a is a 3D version of the inset in Figure 2b where abundance, *m/z*, and mobility have been separately determined for each charge state z. Figure 3b projects Figure 3a into a plane by showing abundance and mass for each charge state. The *z*-resolved mass distributions in (a–b) contain first small quantities of low molecular weight ions that appear at $z = 1$ and 2, and are not particularly informative. The dominant feature for $z \geq 3$ is a narrow peak centered approximately at 6.6 kDa. It includes contributions from charge states $z = 3$–10, peaking at $z = 6$. Excepting the $z = 3$ contribution (originally globular ions), most other charge states in this peak are from "spurious" ions, originally in stretched configurations, which have lost most of their charge on going from the DMA to the mass analyzer. In addition to the main mode at 6.6 kDa, charge states $z = 3$ and higher exhibit a second broader peak centered at characteristic masses given approximately by integer multiples of 6.6 kDa. These more massive ions are associated to aggregates of two or more 6.6 kDa PEG monomers, which result from the relatively large PEG concentrations used in our spraying solution. Some of these aggregates, referred to as multimers, have been identified in Figure 1d and e and Supplementary Figure S3 by a number stating its degree of aggregation and a superscript stating its charge state (i.e, 4^6 denotes four aggregated chains with six charges). Figure 3c represents the mass distribution obtained by summing over all z the z-resolved mass distributions of Figure 3b. Clear peaks at integer factors of the nominal mass distribution (corresponding to the monomer at 6.6 kDa, dimer at 13.2 kDa, trimer at 19.8 kDa, etc.), can be recognized up to charge state z~7, after which the well-defined aggregate peaks are no longer distinguishable.

Several noteworthy features of these multimers are in sharp contrast with the monomer behavior. First, all multimer ions seem to have globular shapes, as they all follow similar patterns to the bands termed globular in Figure 1a. Second, each multimer appears primarily in one charge state, with smaller contributions at one or two higher *z*. A third singular feature is that the multimer abundance (globular regions of Figures 2a and 3a) drops to zero at a sharply defined minimal mass $m^*(z)$, which is in most cases unrelated to the original narrow mass distribution of the aggregates of PEG 6.6 kDa. In other words, $m^*(z)$ is a distinctive characteristic of the charging mechanism of PEG, rather than of the peculiar mass distribution of our sample. This critical mass is reminiscent of a Rayleigh-like condition below which PEG ions have been previously found to cease to be globular [10,18,19]. A liquid drop of density ρ and surface tension γ charged to the Rayleigh limit of water would have a constant m/z^2 of

$$m/z_{Rw}^2 = \rho e^2/(48\pi\gamma\varepsilon_o) \sim 165Da (\text{for room temperature water}), \tag{3}$$

where e is the elementary charge and ε_o the electrical permittivity of vacuum.

Examining the *z*-dependence of this critical mass for our PEG 6.6 kDa, we find that $m^*/z^2 \sim 600$ Da is approximately independent of *z*, a value quite close to that reported earlier [18,19]. This notable feature is demonstrated in Figure S4 of the Supplementary Information by the collapse of the lower end of the various distributions of Figure 3a when represented versus the parameter m/z^2. In other words, while PEG 6.6 kDa monomers exhibit highly charged nonspherical shapes, their multimers not only appear to be mostly spherical but, in addition, take charge states only up to the stability limit for PEG globules. It will be subsequently shown that the DT-MS system is able to transmit substantially nonglobular PEG ion aggregates, so this behavior is partly due to ion activation (charge loss) at the DMA-QStar interface. Although the main apparent implication of Figure 4 turns out to be artificial, the figure still reflects the real fact that the stability of the PEG ions with respect to charge stripping is drastically decreased in nonglobular versus globular configurations.

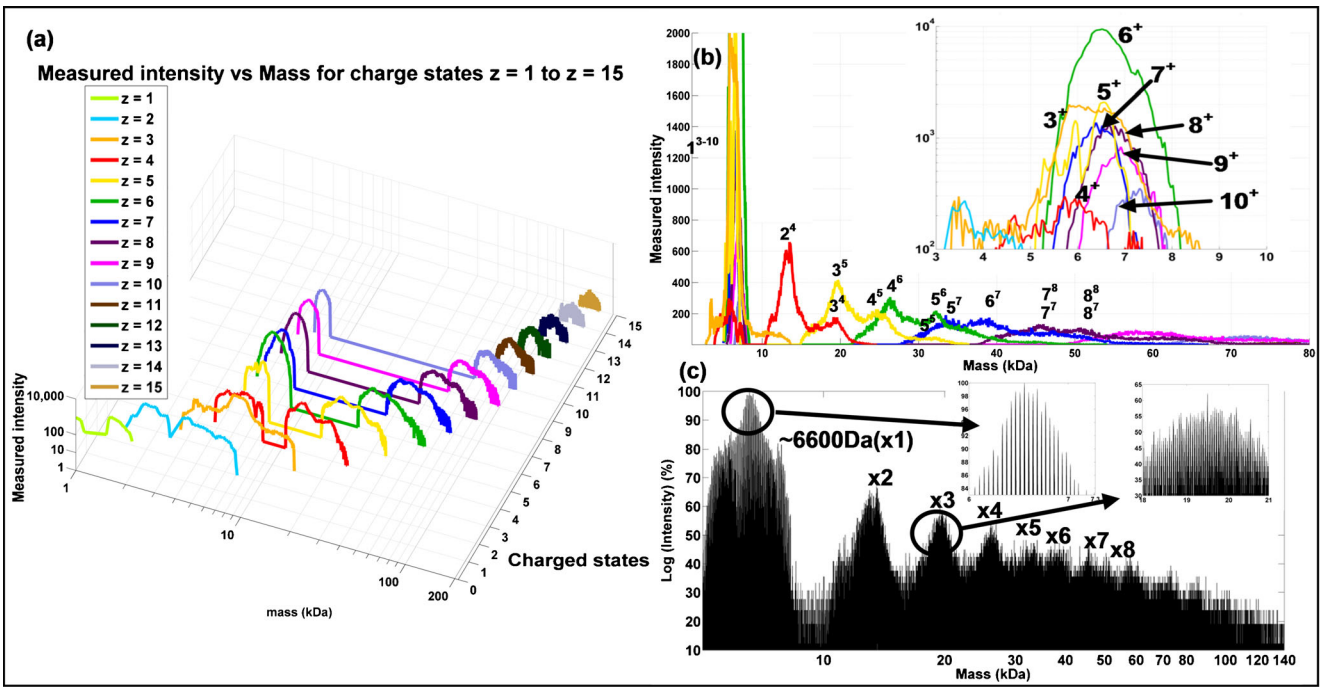

Figure 3. z-Resolved mass distributions for the data of Figure 3a plotted as a function ion mass **(a)**, **(b)**. Mass distribution of the polymer obtained by summing over z the various z-resolved mass distributions **(c)**

Charging Process and Stability of Aggregates

Now that most of the ions have been identified, and that sharp differences in charging patterns have been identified in monomers and multimers, additional mechanistic information on the charging process will be extracted from the data of Figure 1a for PEG 11 kDa in 10 mM $Met_2NH_2^+$. Charging levels are evidently considerably higher than in Eth_3NH^+, with the majority of the ions (red region) being either fully stretched or close to this condition. Furthermore, in spite of the high charge of these PEG ions, the attached $Met_2NH_2^+$ cations have very little tendency to be removed at

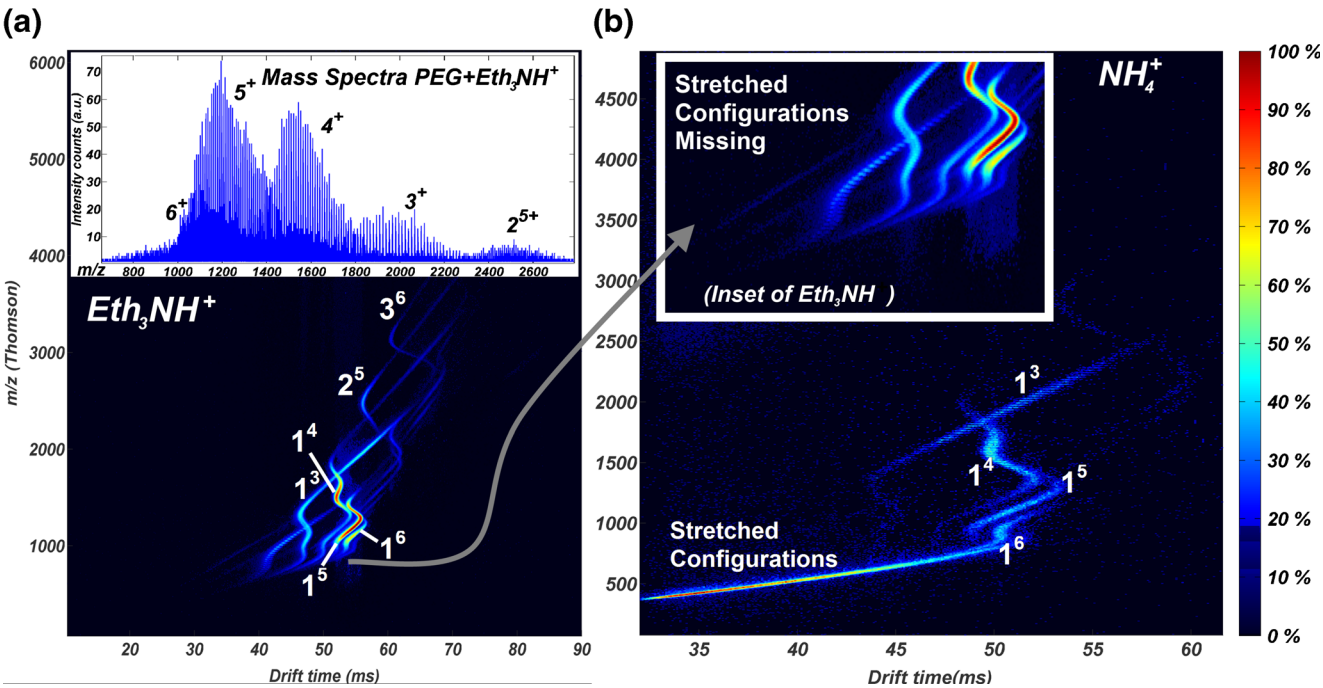

Figure 4. 2D DT-MS spectra of PEG 6 k taken at high resolution with the Indiana drift tube system; **(a)** 3 mg/mL of PEG in Et_3NHF; **(b)** 1 mg/mL of PEG in NH_4Ac buffer

the vacuum interface of the mass spectrometer. Quantitative conversion of the data of Figure 1a into the *z*-selected mass distributions $n_z(m)$ derived in Figure 3 for Eth_3NH^+ is complicated here by the many crossings of the bands. Nonetheless, the set of more abundant regions (the vicinity of the mean of the mass distributions) corresponding to various charge states of the monomers, dimers, etc., is highly informative. For example, Figure 1c displays up to charge state 14 in the fully stretched region, where the largest *m/z* increment between two adjacent peaks corresponds to ~3 Da (*m/z* = 44 Da/14~3.14 Da). Aside from the stretched region, by far the most abundant series is that of monomers, carrying 5, 6, 7, 8, 9 charges, and labeled 1^5, 1^6, 1^7, 1^8, 1^9, 1^{10} in Figure 1d. Also marked in Figure 1e are the dimer region from 2^7 to 2^{11} and the trimer region 3^8 to 3^{12}. Particularly interesting is also the band for $z = 5^+$, showing a relatively weak signal in the region between 2500 and 4000 *m/z* (12.5 kDa<m<20 kDa). This is the domain between the monomer and the dimer, which is in this case fully globular and labeled 2^5. The sixth charge state, 6^+, can be followed with some limited interruptions, with its dimeric contribution including globular as well as nonglobular configurations.

On a more quantitative note, the well-resolved 1^9 ions labeled in Figure 1d correspond to m/z^2~111. Accordingly, the monomer forms fully stretched ions charged well above the Rayleigh limit of water (~165). This level of supercharging is a well-known characteristic of PEG cationized with small ions such as H^+[23,25,26], Na^+ [18,19,27], NH_4^+ [19,23], and Cs^+ [20,21].

The situation of the multimer ions in the $Met_2NH_2^+$ buffer seems at first sight to be substantially different from that in the Eth_3NH^+ buffer, as the dimers now adopt nonglobular configurations, including charge states up to z = 11 (or more). However, as already noted, this difference is artificial. Note first that all the nonglobular multimers in $Met_2NH_2^+$ are still far from fully stretched forms, and can be seen to charge at most below the Rayleigh limit of a water drop having the same volume as the PEG molecule. This point is difficult to prove based on complete *z*-resolved mass distributions (such as those of Figure 3 for PEG 6.6 k), but can nonetheless be established based on the ion abundance at the peak of the distributions, marked in Figure 1d and e. The ion intensity can be seen to be relatively unchanged for the dimer in Figure 1e when *z* increases from 2^7 up to 2^{11}. This is followed by a drastic intensity reduction at $z = 12$, hardly distinguishable from the complete disappearance of this charge state. The middle of the 2^{11} peak corresponds to the mean mass of the distribution (~2 × 11 kDa), with m/z^2~ 181 Da. This is slightly below the Rayleigh limit (3) of a water drop. In contrast, m/z^2 for 2^{12} would be 152 Da, slightly above this Rayleigh limit. The conspicuous absence of 2^{12} therefore suggests that the dimer charges at most to the Rayleigh limit of water. This is supported by the fact that the highest charged state for the monomers is at least 14 (see Figure 1e), so the ion 2^{14} could in principle be formed from the charging mechanism perspective. Whether 2^{13} and 2^{14} are initially produced but then the two constituents (monomeric chains) are separated because of strong Coulombic repulsion remains to be settled. Similarly for the trimers, ion intensity is relatively unchanged from 3^8 to 3^{12}, all charge states having narrow distributions around the mean mass (~3 × 11 kDa). In this case, 3^{12} can be surely distinguished and perhaps 3^{13} is present, but 3^{14} seems absent. The respective m/z^2 are 229, 195, and 168 Da, the latter (for 3^{14}) being very close to the Rayleigh limit of water. A summary of these observations from the DMA-MS is included in Table 1.

We have also reexamined the behavior of PEG in Eth_3NH^+ solutions in the drift tube IMS (DT-IMS) with results shown in Figure 4a. Charge states are now restricted to the range $z \leq 6$ (rather than $z \leq 14$ in Figure 1a), whereas charge stripping between the IMS and the MS is greatly reduced. This is qualitatively as expected, since charge stripping now takes place upstream of the IMS in the pressure differential region, resulting in lower charge states but with fewer and less prominent anomalously located bands (though some are clearly visible in the inset of Figure 4a). Less expected was the observed survival of highly elongated monomeric chains, almost down to the fully stretched configuration. For instance, Figure 4a demonstrates a measurable signal of z = 7 ions at 840 Thomsons, with $m/z^2 = 120$ carrying a charge well above the Rayleigh limit of water. We believe most of these considerably stretched configurations are not original, but are rather derived by charge stripping from originally fully stretched ions. The apparently milder process of ion entry in the DT-MS system (Figures 4a) versus the Q-Star (Figures 2a) may be partly due to the relatively stronger RF of the QStar. Examination of the maximal charge levels achieved by dimers and trimers present in Figure 4a confirms the prior conclusions that all multimer ions are below the Rayleigh limit of water. Interestingly, this point applies also to PEG ions carrying very small cations, as demonstrated in Figure 4b, based on a NH_4^+ buffer.

Splitting Aggregated Chains by IMS-IMS

We have used the IMS-IMS capability of the drift tube apparatus to study the stability of aggregated chains formed by several PEG 6KDa units cationized with NH_4^+. Only the ions contained in a selected small drift time window are allowed to go from a first drift region (approximately 1 m) into a second one (approximately 2 m). Prior to releasing the ions into the second drift region, a controllable voltage difference is applied between the last two consecutive lenses (IA2 in Supplementary Figure S1b) of the funnel (F2 in Supplementary Figure S1b), which are spaced 0.3 cm apart. When sufficient voltage is applied, aggregated chains of PEG may be dissociated, enabling the study of their products through IMS-MS. Figure 5 shows the products from two drift windows, labeled (a) [54–59 ms] and (b) [59–64 ms] (see Figure S4 and Figure S5 of the Supplementary Information for higher resolution and details). For window (a),

Table 1. Charging Characteristics of PEG Monomers and Aggregates in Met_2N^+ and Eth_3A^+ Buffers

Ion	Shape	ES charge	MS charge
Monomer/$Met_2NH_2^+$	Fully stretched	$>z_{R\text{-}w}$[a]	$>z_{R\text{-}w}$[a]
Aggregate/$Met_2NH_2^+$	Partly stretched	$<z_{R\text{-}w}$[a]	$<z_{R\text{-}w}$[a]
Monomer/Eth_3NH^+	Fully stretched (charge lost in interface)	$>z_{R\text{-}w}$[a]	$<z_{R\text{-}w}$[a]
Aggregate/Eth_3NH^+	Globular	$<z_{R\text{-}PEG}$[b]	$\leq z_{R\text{-}PEG}$[b]
Aggregate/Eth_3NH^+	Partly stretched (charge lost in interface)	$<z_{R\text{-}w}$[b]	$\leq z_{R\text{-}w}$[b]

[a]Rayleigh limit of a water drop of the same volume as the PEG ion.
[b]Maximum charge held by a PEG globule of given mass.

raising the voltage between the lenses to 200 V splits the aggregate labeled 2^5 into two globular monomers denoted 1^3 and 1^2. The average mass of the parent 2^5 chains is slightly below 12,000 Da (2300 × 5 = 11,500 Da), while those of the product monomers are 1850 × 3 = 5550 and 3000 × 2 = 6000 Da. A key observation is that the parent ions below the kink in the band can be fragmented, whereas those above the kink cannot. The stable ions above the kink are globular, whereas the labile ions below the kink include a protruding piece of the chain carrying one charge external to the globule (sketch at the bottom of the second pane of Figure 5) [18]. Note that this collisional activation does not detach the cation from the protrusion, but rather helps disentangle and separate the two monomers. This fragmentation therefore looks very much as an extrusion process, where the electric field pulls out the partially external monomer, whereas the energy deposited on the larger globule helps overcome the activation barrier needed to complete the extrusion process. The reality of the Fenn-Consta extrusion process [3–6] is therefore strongly confirmed, if not for drawing the chain out of a drop of solvent, certainly for pulling it out of a melt of pure polymer (the dimer). It is worth noting that the extrusion process involves not just two steps, but a multitude of activated processes in series, since multiple charges need to be serially pulled out of the solvent. However, the subsequent steps surely have decreasing activation energies, given the increasing electrostatic pull from the ions already external to the drop. The conventional step for evaporating a bare ion from the surface of a solvent drop involves activation energies in the range of 2 eV. One would therefore expect that the analogous step of escape of the first cation tied to the polymer backbone would be even more endothermic. Were it not for the peculiar instability of charged PEG ions, which naturally prepares them in a configuration having overcome the first activated step, it would be hard to conceive an experimental method to measure the activation energy of the extrusion process, which plays an important role in Consta and Chung's extrusion calculations [4]. Their model could conceivably be applied to PEG aggregates, and the corresponding activation energy could also be measured by techniques akin to those used here.

The second drift window, (b), shows first that the globular ions 3^5 and 2^4 are also stable. As seen from the survival of the 3^6 aggregate (labeled in the figure) below the kink, we find that 200 V do not suffice to detach a monomer from a trimer having just one external charged appendix.

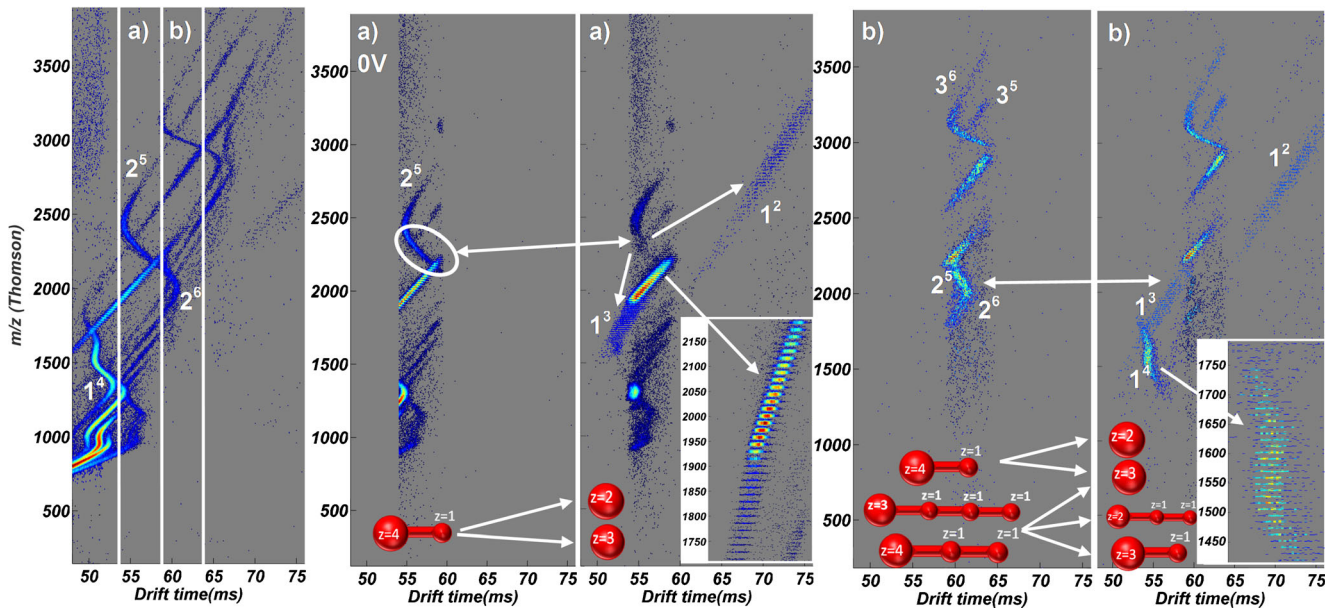

Figure 5. IMS-IMS of sample PEG 6 kDa in an NH_4^+ buffer for two different drift windows. **(a)** After enough energy, aggregate 2^5 separates into the two globules 1^3 and 1^2. **(b)** Similarly, aggregates 2^5 and 2^6 in the transition regime separate into 1^2 and 1^3, and 1^2 and 1^4 (or perhaps two 1^3), respectively

The contrast with the fate of the 2^5 parent fragmented in panel (a) shows that the energy required to extrude a fixed chain with a single external charge out of a globule increases with globule size. In contrast, the kinks formed by 2^5 and 2^6 at the left of the window can be separated into monomers. The 2^5 aggregate is disentangled in a way similar to that previously shown in window (a), although in lower abundance, forming the two globular monomers 1^3 and 1^2. Even more remarkable is the fragmentation pattern of the parent dimer 2^6 in the region above the kink at ~2000 *m/z*, which is formed by a linear appendix containing two or three charges and a globule with the remaining four or three charges (depending on whether the aggregate is above or below the kink) [18], as sketched in the lower part of the figure. Two among the possible paths of fragmentation are observed: $2^6 \rightarrow 1^3+1^3$, and $2^6 \rightarrow 1^2+1^4$, the dominant fragments seem to correspond to the second asymmetric breakup, although part of the 1^3 and 1^2 may originate from 2^5 rather than 2^6. The 1^4 product restructures itself and falls into an "s" shaped transition region [18] reminiscent of that of the original 1^4 monomer formed directly in the electrospray (see full contour plot on the left of Figure 5 and on its right inset), which is formed by a globule including either two or three charges and an appendix with the balance of charge. We have confirmed from the raw data that the 1^4 chain product has the same cross section as the original 1^4 chain, and that the products 1^2 and 1^3 have the same structure as the original 1^2 and 1^3 ions.

The Effect of Cation Size on the Level of Charge Stripping

Figure 6 shows 8 DMA-MS spectra for PEG 11 kDa, ordered by ion size and ignoring the effect of charge delocalization. One can observe a clear trend for increased loss of charge in stretched chains as the cation size is increased (see a larger version of the Met_3NH^+ figure in the Supplementary Information, Figure S5). H^+ and NH_4^+ exhibit very little charge stripping, whereas $Met_2NH_2^+$ already shows a small but observable charge loss (see inset) in fully stretched ions. Substantial charge stripping arises for stretched ions in $Eth_2NH_2^+$ and Met_3NH^+, although most of the pseudo-charge states can be corrected to match closely the $Met_2NH_2^+$ spectra. The correction for Eth_3NH^+ becomes more difficult, as even the nonglobular ions charged modestly above the limit of stability for PEG (globular to stretched transition) are losing charge. The $Prop_3NH^+$ spectrum on the contrary shows a much weaker trend to form highly stretched configurations, identifiable through a relatively weak signal from pseudo-charge states. Some original globular-to-stretched configurations can still be observed at high mass and low mobility, decisively demonstrating that the rest of the nonglobular configurations have disappeared because of violent charge loss events.

Finally, the largest cation, But_4N^+, clearly shows that charge may be lost even from globular configurations. In this case, the complete absence of nonglobular ions indicates that the cation does not bind well to the chain, not even under atmospheric conditions, similarly as recently found in negatively ionized PEG in a water/methanol solution containing dimethylammonium formate [28]. Notice several charge loss events taking place from globular parent ions, to the point that charge state 4 loses up to three charges. It is apparent that most of these charges are not in the interior of the PEG globule, being rather weakly held on its surface.

Increasing the declustering potential similarly enhances the charge stripping effect, as seen in Figure S6 of the Supplementary Information for PEG 11 kDa seeded with Eth_3NH^+. In this case, on raising the declustering potential from 0 to 200 V, charge stripping increases substantially, not only for the globular configurations but also for the stretched pseudo charge states, leaving the singly charged ions as the most abundant in the mass spectrum (left of the figure).

Discussion

The Ionization Mechanism

The Role of the Charging Ion Most buffers produce comparably large initial monomer charge states (superRayleigh), which survive the mobility measurement under ambient conditions. These charge levels are comparable to those previously observed for PEG ions attached to smaller and strongly held cations such as Na^+, NH_4^+, Cs^+, and H^+ [18–27]. Note, however, that this fact is obscured by charge stripping in most existing IMS-MS instruments, including the DT-MS, where charge and mobility determination takes place after the ions have been subject to a relatively harsh introduction into the vacuum system. Indeed, the main difference between Eth_3NH^+ and the smaller cations is really not in the ionization process but in the different ability of different ions to remain bound to the PEG chain during the relatively violent process of entry into the mass spectrometer. This ability depends on the nature of the buffer and the MS interface, but even for the weakly bound Eth_3NH^+, the charge under atmospheric conditions at temperatures of ~40°C is stable through characteristic times long enough to complete our mobility measurement with a DMA (100 to 200 μs). This level of stability is clear from the sharp mobility peaks seen for the metastable ions in Figure 2a. The fact that Eth_3NH^+ is partially removed at the vacuum interface and smaller cations are not, is therefore irrelevant to the electrospray ionization mechanism.

Ion Evaporation Monomers are singular in that they form as fully elongated ions with $z>z_{Rw}$ (Equation 3), whereas multimer ions do not stretch so far and seem to be charged below z_{Rw}. Beyond this apparent difference between monomers and dimers, what is significant is that the many monomers observed with $z>z_R$ cannot be formed as charged

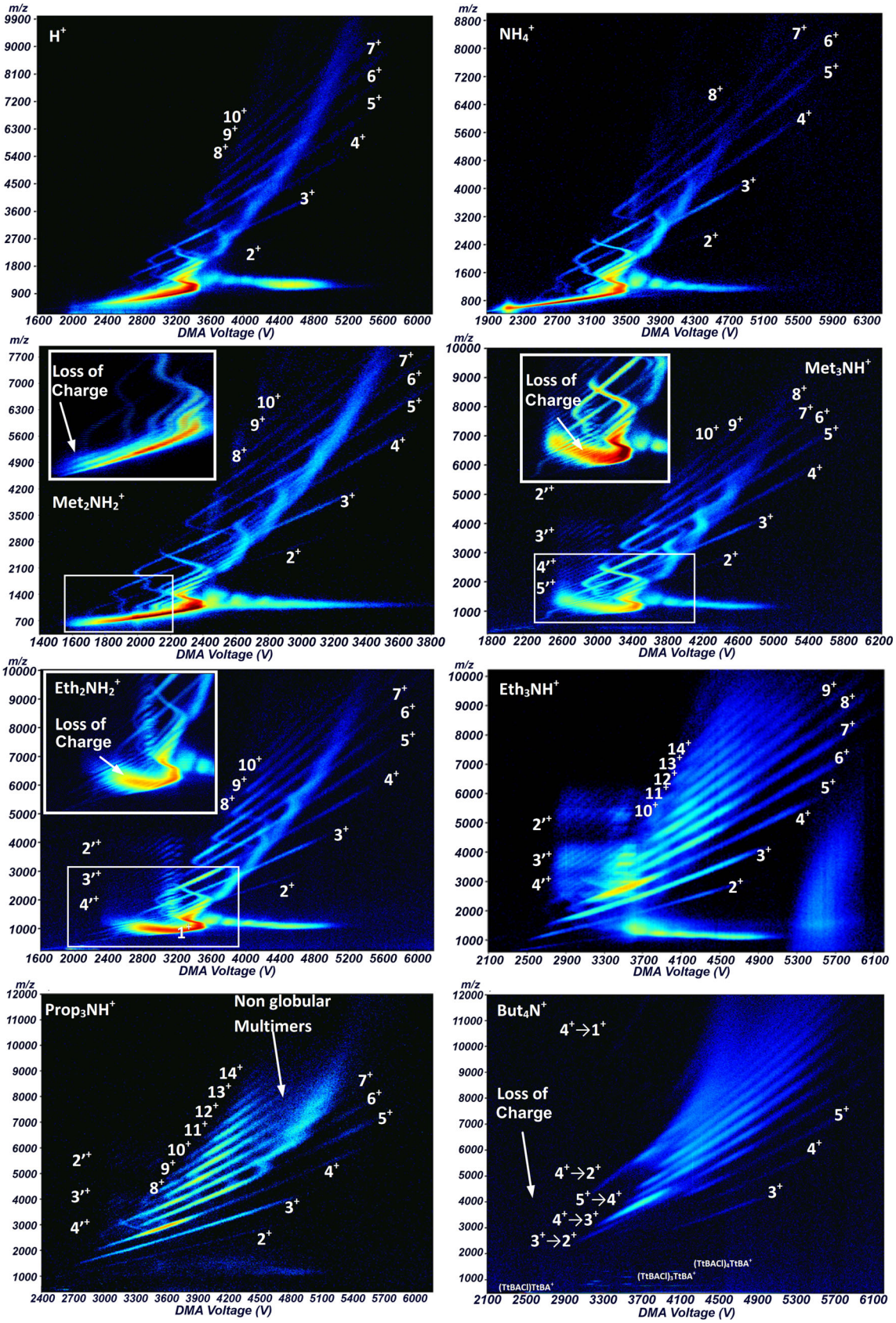

Figure 6. PEG 11 kDa seeded with eight different cations in a 50/50 water methanol solutions. The cations, ordered by increasing size are: H^+, NH^{4+}, $Met_2NH_2^+$, Met_3NH^+, $Eth_2NH_2^+$, Eth_3NH^+, $Prop_3NH^+$, But_4N^+. Insets are provided where the charge loss is difficult to observe

residues from spherical drops. Either they are charged residues from nonspherical drops held together by the polymer (a possibility not considered here), or they must escape from the drop prior to its complete drying. This latter mechanism is evidently a special form of ion evaporation, details of which will be considered later. Irrespective of these details, the ionization mechanism producing supercharged ions ($z>z_R$) acts equally on 6 kDa and 12 kDa chains and should, therefore, be effective also with dimers of 6 kDa chains. Accordingly, the reason why fully elongated multimers are not observed must be that the several monomers are torn apart by Coulombic forces, either during the ion evaporation process or shortly after in the gas phase. Either way, in spite of the appearances, the basic mechanism of ionization does not distinguish between monomers and aggregates.

Charge Residue Mechanism A second important point to note is that although the monomer ions may be highly charged, many monomers are weakly charged. This is evident in Figure 3b, where the monomers span charge states $3 \leq z \leq 10$. The scantily charged monomers must be formed as charged residues from small drops containing just one PEG molecule. The charged residue mechanism evidently applies also to multimer ion formation, showing again no fundamental difference in the production of monomers and multimers. The process would then start with a just-formed globular dried polymer residue charged to $z \leq z_{Rw}$. Because this initial z greatly exceeds $z_{R\text{-}PEG}$ (effective Rayleigh limit for PEG with $\rho = 1115$ kg/m3 and $\gamma = 45$ dyn/cm), rapid ejection of one or two charged appendices from the PEG globule will rapidly follow, ending in one of the stable nonglobular structures sketched in Figure 5 or [18]. The only difference between dimers and monomers would then be associated to the stability of the dimer rather than to the mechanism of ionization. Although fully elongated dimers are not stable with respect to Coulombic stretching, we have observed stable dimers composed of a central globule including only a few charges, with the rest of the charge being carried in one or two fully stretched linear appendices. It is apparent that the key to the stability of these relatively elongated dimers (versus their unstable fully elongated counterparts) rests in the fact that each of the several charges trapped within the multiply charged globule belong to different chains, therefore providing sufficient binding energy to withstand the pull from the external linear pieces, at least at room temperature. The tandem IMS approach used in this article could be extended to systematically study the magnitude of this binding energy.

Is PEG Ion Evaporation an Extrusion Process? The main difference between the evaporation of a long multiply charged polymer ion from a liquid surface and the more familiar evaporation of small ions is that polymer evaporation involves a multi-stage process: first the usual ion evaporation releasing a first charged piece of the chain, and then the gradual extrusion of the whole chain away from the liquid. The qualitative appeal of this picture (as proposed by Fenn), reinforced by the quantitative modeling by Consta and colleagues, is already quite persuasive [3–6]. The reality of this multi-step process is further reinforced by our experiments on the fragmentation of PEG dimers. There, in the absence of an external charged appendix for the field to pull, one chain cannot be drawn from the melt (the dimer) in spite of the strong electric field, and the substantial collisional activation applied. Yet, once the first step is implemented (externalization of the first charge), extrusion proceeds readily. Although our observation does not apply directly to a chain in a charged drop, it indicates that the first step involves substantially higher activation energy than the subsequent extrusion. This point is also expected intuitively, since most of the extrusion work (both in a solvent and in a polymer melt) must be associated to pulling the subsequent charges (rather than the neutral chain) from the liquid. But since the electrostatic pull from the field increases steadily as more charges have been extruded, removal of the n^{th} charge should take a smaller effort than for the prior one. This does not mean that extraction of the second and subsequent charges is a downhill process. The opposite is, in fact, proven by our collision activation experiments. The observation of two ionization mechanisms is also consistent with the extrusion model. The high charge states would originate from ions extruded fully, whereas the nonglobular multimers with a segment sticking out would presumably result from incomplete extrusion events interrupted by drying of the drop.

Besides the simulation work already cited [4–7], further support for the extrusion model is provided by related biopolymer ionization simulations [29,30] aimed at explaining the often observed asymmetric fragmentation of protein complexes under collision activation. In this model [29], while one monomer is extruded from the aggregate as an elongated chain, charge is preferentially transferred to it, leading to its escape from the aggregate with a substantial fraction of the initial charge. This asymmetry is sometimes extreme. For instance, analyzing the original data from [31], we find that the tetradecamer GroEl (m~0.8 MDa) carrying up to 81 charges (mean 76) fragments producing a dodecamer with up to 52 charges (mean 42) and two monomers, one of them with up to 37 charges (mean 29) [31]. Therefore, one out of the 14 monomers in the initial assembly departs carrying up to 45% of the total charge! The breakup of protein dimers analyzed in [30] indicates that the subunit carries between 50% and 65% of the total charge. This partitioning is comparable to what we observe in our partially unfolded PEG dimer 2^6 , whose product 1^4 carries 66% of the initial charge. These analogies are evidently of great interest, even though our observations differ from all prior protein complex fragmentation studies in the far greater malleability of PEG, and the fact that we start with a partially unfolded aggregate.

Conclusions

We have used two complementary IMS-MS techniques to investigate the charge states of PEG ions produced by electrospraying their solutions from various buffers with the following findings

(1) Although cations of increasing size result in decreasing charge levels in the MS detector, this behavior is an artifact of the violent process of ion entry into the mass spectrometer, where some of the charge bound to highly stretched regions of the polymer is stripped. Except for the largest and most weakly bound cations, the level of original charging achieved in the electrospray region is very high for all cations studied: as high as permitted by the strong Coulombic repulsion arising even in fully stretched configurations [27]. Charge stripping is stronger for the larger and more weakly bound cations such as Et_3NH^+, and is relatively unimportant for small ions such as H^+ and NH_4^+. Charge stripping decreases dramatically for globular polymer structures, indicating that the most labile ions are those attached to highly stretched linear pieces of the chain.

(2) Single-chain polymer ions are found in very high charge levels exceeding z_{Rw} (the Rayleigh limit of a water drop of the same volume as the PEG molecule), whereas multimer ions incorporating two or more individual chains always charge below z_{Rw}. Rather than from the existence of different ionization mechanisms for monomers and multimers, this difference results from the inability of two highly charged chains to remain together against the Coulombic forces pulling them apart.

(3) Highly stretched single chains with $z>z_{Rw}$ levels have been previously observed to be the dominant species in electrosprays of various polymers, even up to polymer masses of several million [32]. However, at the high PEG concentrations used here in the electrosprayed solution, a substantial fraction of the PEG sample forms globular and incompletely stretched ions, some containing only one chain, others including several chains. This behavior points out to the coexistence of two ionization mechanisms: ion evaporation yielding monomers with $z>z_{Rw}$, and Dole's mechanism giving rise to monomeric and multimeric species, all with $z<z_{Rw}$.

(4) Collision activation studies of electrosprayed ions formed by two PEG chains show that at available energies of 200 V, globular dimers cannot be broken up into their two constituents, but some nonglobular dimers dissociate readily. This behavior is reminiscent of the substantially smaller stability towards charge stripping previously noted for nonglobular polymer ions. However, in the present case, collision activation leads not to charge loss but to dimer dissociation. The observed drastic facilitation of aggregate dissociation brought about by the presence of a small charged linear branch of the chain external to the main dimer body suggests strongly that the mechanism of dimer dissociation is the same Fenn-Consta extrusion process previously postulated for multiply charged chain evaporation from a solvent drop.

(5) The analogy between the *extrusion process* observed here in the dissociation of nonglobular PEG dimer ions and that previously postulated for electrospray ionization of polar chains provides additional (though indirect) evidence in support of this hypothetical ionization mechanism.

Acknowledgments

The authors thank Applied Biosystems and SEADM for their loan of the IMS-MS facility, (http://www.eng.yale.edu/DMAMSfacility/), Yale's W. M. Keck Center for hosting it, Bruce Thomson for his guidance on mass spectrometry and Q-Star MS issues, and Juan Fernández García (Yale) and Alejandro Casado (SEADM) for their key contributions to the data inversion routines. C.L. acknowledges the Ramon Areces Fellowship for its support. Following Yale University rules, J.F.M. declares that he has a personal interest in the company SEADM manufacturing the differential mobility analyzer used in this research.

References

1. Cook, K.D.: Electrohydrodynamic mass spectrometry. Mass Spectrom. Rev **5**, 467–519 (1986)
2. Iribarne, J.V., Thomson, B.A.: On the evaporation of small ions from charged droplets. J Chem Phys **64**, 2287–2294 (1976)
3. Fenn, J.B., Rosell, J., Meng, C.K.: In electrospray ionization, how much pull does an ion need to escape its droplet prison? J Am Soc Mass Spectrom **8**, 1147–1157 (1997)
4. Chung, J.K., Consta, S.: Release mechanisms of poly(ethylene glycol) macroions from aqueous charged nanodroplets. J Phys Chem B **116**, 5777–5785 (2012)
5. Ahadi, E., Konermann, L.: Modeling the behavior of coarse-grained polymer chains in charged water droplets: implications for the mechanism of electrospray ionization. J Phys Chem B **116**, 104–112 (2012)
6. Konermann, L., Ahadi, E., Rodriguez, A.D., Vahidi, S.: Unraveling the mechanism of electrospray ionization. Anal Chem **85**, 2–9 (2013)
7. Consta, S., Malevanets, A.: Manifestations of charge induced instability in droplets effected by charged macromolecules. Phys Rev Lett **109**, 148301 (2012)
8. Hogan, C.J., Fernández de la Mora, J.: Tandem ion mobility-mass spectrometry (IMS-MS) study of ion evaporation from ionic liquid-acetonitrile nanodrops. Phys. Chem., Chem Phys **11**, 8079–8090 (2009)
9. Dole, M., Mack, L., Hines, R., Mobley, R., Ferguson, L., Alice, M.: Molecular beams of macroions. J Chem Phys **49**, 2240–2249 (1968)
10. Rayleigh, L.: On the equilibrium of liquid conducting masses charged with electricity. Philos. Mag. **14**, 184 (1882). The Theory of Sound, Macmillan, London, Vol. 2 (1878); The Theory of Sound, 2nd ed., Macmillan, London (1894); The Theory of Sound , Dover, New York, reprint (1945)
11. Fernández de la Mora, J.: Electrospray ionization of large multiply charged species proceeds via Dole's charged residue mechanism. Anal Chim Acta **406**, 93–104 (2000)
12. Rus, J., Moro, D., Sillero, J.A., Royuela, J., Casado, A., Fernández de la Mora, J.: IMS-MS studies based on coupling a differential mobility analyzer (DMA) to commercial API-MS systems. Int J Mass Spectrom **298**, 30–40 (2010)
13. Ude, S., Fernández de la Mora, J.: Molecular monodisperse mobility and mass standards from electrosprays of tetra-alkyl ammonium halides. J Aerosol Sci **36**, 1224–1237 (2005)

14. Hoaglund, C.S., Valentine, S.J., Sporleder, C.R., Reilly, J.P., Clemmer, D.E.: Three-dimensional ion mobility/TOFMS analysis of electrosprayed biomolecules. Anal Chem **70**, 2236–2242 (1998)
15. Koeniger, S.L., Merenbloom, S.I., Valentine, S.J., Jarrold, M.F., Udseth, H., Smith, R., Clemmer, D.E.: An IMS-IMS Analogue of MS-MS. Anal Chem **78**, 4161–4174 (2006)
16. Merenbloom, S.I., Koeniger, S.L., Valentine, S.J., Plasencia, M.D., Clemmer, D.E.: IMS-IMS and IMS-IMS-IMS/MS for separating peptide and protein fragment ions. Anal. Chem **78**, 2802–2809 (2006)
17. Counterman, A.E., Valentine, S.J., Srebalus, C.A., Henderson, S.C., Hoaglund, C.S., Clemmer, D.E.: High-order structure and dissociation of gaseous peptide aggregates that are hidden in mass spectra. J Am Soc Mass Spectrom **9**, 743–759 (1998)
18. Larriba, C., Fernández de la Mora, J.: The gas phase structure of Coulombically stretched polyethylene glycol ions. J. Phys Chem. B **116**, 593–598 (2012)
19. Ude, S., Fernández de la Mora, J.: Charge-induced unfolding of multiply charged polyethylene glycol ions. J Am Chem Soc **126**, 12184–12190 (2004)
20. Trimpin, S., Clemmer, D.E.: Ion mobility spectrometry/mass spectrometry snapshots for assessing the molecular compositions of complex polymeric systems. Anal Chem **80**, 9073–9083 (2008)
21. Trimpin, S., Plasencia, M., Clemmer, D.E.: Resolving oligomers from fully grown polymers with IMS-MS. Anal Chem **79**, 7965–7974 (2007)
22. Wyttenbach, T., Bowers, M.T.: Gas-phase conformations: the ion mobility/ion chromatography method. Mod. Mass Spectrom. **225**, 207–232 (2003)
23. Larriba, C., Hogan, C.J.: Free molecular collision cross section calculation methods for nanoparticles and complex ions with energy accommodation. J Phys Chem A **117**, 3887–3901 (2013)
24. Consta, S., Malevanets, A.: Classification of the ejection mechanism of charged macromolecules from liquid droplets. J Chem Phys **138**, 044314 (2013)
25. Huang, L., Gough, P.C., DeFelippis, M.R.: Characterization of poly(ethylene glycol) and PEGylated products by LC/MS with postcolumn addition of amines. Anal Chem **81**, 567–577 (2009)
26. Bagal, D., Zhang, H., Schnier, P.D.: Gas-phase proton-transfer chemistry coupled with TOF mass spectrometry and ion mobility-MS for the facile analysis of poly(ethylene glycols) and PEGylated polypeptide conjugates. Anal Chem **80**, 2408–2418 (2008)
27. Wong, S.F., Meng, C.K., Fenn, J.B.: Multiple charging in electrospray ionization of polyethylene glycols. J Phys Chem **92**, 546–550 (1988)
28. Criado, E., Fernández-García, J., Fernández de la Mora, J.: Mass and charge distribution analysis of large polyethylene glycol chains by negative electrospray ion mobility mass spectrometry (NES-IMS-MS). Anal Chem **85**, 2710–2716 (2013)
29. Konermann, L., Rodriguez, A.D., Liu, J.: On the formation of highly charged gaseous ions from unfolded proteins by electrospray ionization. Anal Chem **84**, 6798–6804 (2012)
30. Sciuto, S.V., Liu, J., Konermann, L.: An electrostatic charge partitioning model for the dissociation of protein complexes in the gas phase. J Am Soc Mass Spectrom **22**, 1679–1689 (2011)
31. Hogan, C., Ruotolo, B., Robinson, C., Fernandez de la Mora, J.: Tandem differential mobility analysis-mass spectrometry reveals partial gas-phase collapse of the GroEL complex. J. Phys Chem. B **115**, 3614–3621 (2011)
32. Nohmi, T., Fenn, J.B.: Electrospray mass spectrometry of poly(ethylene glycols) with molecular weights up to five million. J Am Chem Soc **114**, 3241–3246 (1992)